

Fermi National Accelerator Laboratory

FERMILAB-Conf-95/030-E

DØ

The DØ Detector Upgrade

Alan D. Bross
For the DØ Collaboration
Fermi National Accelerator Laboratory
P.O. Box 500, Batavia, Illinois 60510

February 1995

Submitted to Proceedings of the *4th International Conference on Advanced Technology and Particle Physics*,
Como, Italy, October 3-7, 1994

Disclaimer

This report was prepared as an account of work sponsored by an agency of the United States Government. Neither the United States Government nor any agency thereof, nor any of their employees, makes any warranty, express or implied, or assumes any legal liability or responsibility for the accuracy, completeness, or usefulness of any information, apparatus, product, or process disclosed, or represents that its use would not infringe privately owned rights. Reference herein to any specific commercial product, process, or service by trade name, trademark, manufacturer, or otherwise, does not necessarily constitute or imply its endorsement, recommendation, or favoring by the United States Government or any agency thereof. The views and opinions of authors expressed herein do not necessarily state or reflect those of the United States Government or any agency thereof.

The DØ Detector Upgrade *

Alan D. Bross
for the DØ Collaboration

Fermi National Accelerator Laboratory, Batavia, IL 60510 USA

The Fermilab collider program is undergoing a major upgrade of both the accelerator complex and the two detectors. Operation of the Tevatron at luminosities upwards of ten times that currently provided will occur in early 1999 after the commissioning of the new Fermilab Main Injector. The DØ upgrade program has been established to deliver a detector that will meet the challenges of this environment. A new magnetic tracker consisting of a superconducting solenoid, a silicon vertex detector, a scintillating fiber central tracker, and a central preshower detector will replace the current central tracking and transition radiation chambers. We present the design and performance capabilities of these new systems and describe results from physics simulations that demonstrate the physics reach of the upgraded detector.

1. Introduction

The original proposal for the DØ detector was made in 1983 and put forward a coherent view that, in order to fully exploit the physics opportunities at the Tevatron, high precision detection of electrons and muons, quarks and gluons materialized as jets, and neutrinos inferred from missing E_T were an absolutely necessity. The great success of DØ's first collider run has shown the validity of both this idea and how these concepts were applied to the detector's design and construction. The evolving Tevatron upgrade program has, however, already taken the detector well beyond the luminosity for which it was designed, $10^{30} \text{cm}^{-2} \text{sec}^{-1}$ [1]. In the era of the Main Injector at Fermilab, the Tevatron's luminosity will be further upgraded, approaching $1 - 2 \times 10^{32} \text{cm}^{-2} \text{sec}^{-1}$. This will be accompanied by an initial decrease in the bunch crossing time from the current 3.5 μsec to 396 ns and then to a final value of 132 ns. In order to continue to take full advantage of the physics opportunities offered at the Tevatron, while dealing with a shorter bunch crossing time and increased radiation damage in the tracking systems, a major upgrade of the DØ detector is underway. [2]

The DØ upgrade program will augment some

components of the current detector system while completely replacing others. The calorimeter, trigger, data acquisition, and muon systems will be upgraded to allow for operation at the luminosity indicated above. However, the increased radiation environment presented by the upgraded Tevatron will make the operation of DØ's vertex chamber, central and forward tracking systems, and central transition radiation detector problematic. In addition, the rather long drift times ($\approx 1 \mu\text{sec}$) characteristic of these gaseous detectors severely compromises their operation at short bunch crossing times. For these reasons, the upgrade will completely replace these systems.

The upgraded tracking system's design has been motivated by a number of goals: the addition of a magnetic field for momentum measurement and charge sign determination; improved speed and granularity; tracking to a pseudorapidity (η) of ± 3 ; level one tracking trigger; good electron identification; secondary vertex measurement of b -quark jets in top quark and bottom quark physics studies; and radiation hardness. The existing non-magnetic tracking system will be replaced by a high resolution magnetic tracking and vertexing system consisting of a 2 Tesla superconducting solenoid, an outer scintillating fiber tracker, and an inner silicon tracker. In addition, a preshower detector will be mounted outside the coil. Figure 1 shows a r-z view of the DØ

*This work supported by the U.S. Department of Energy and the U.S. National Science Foundation

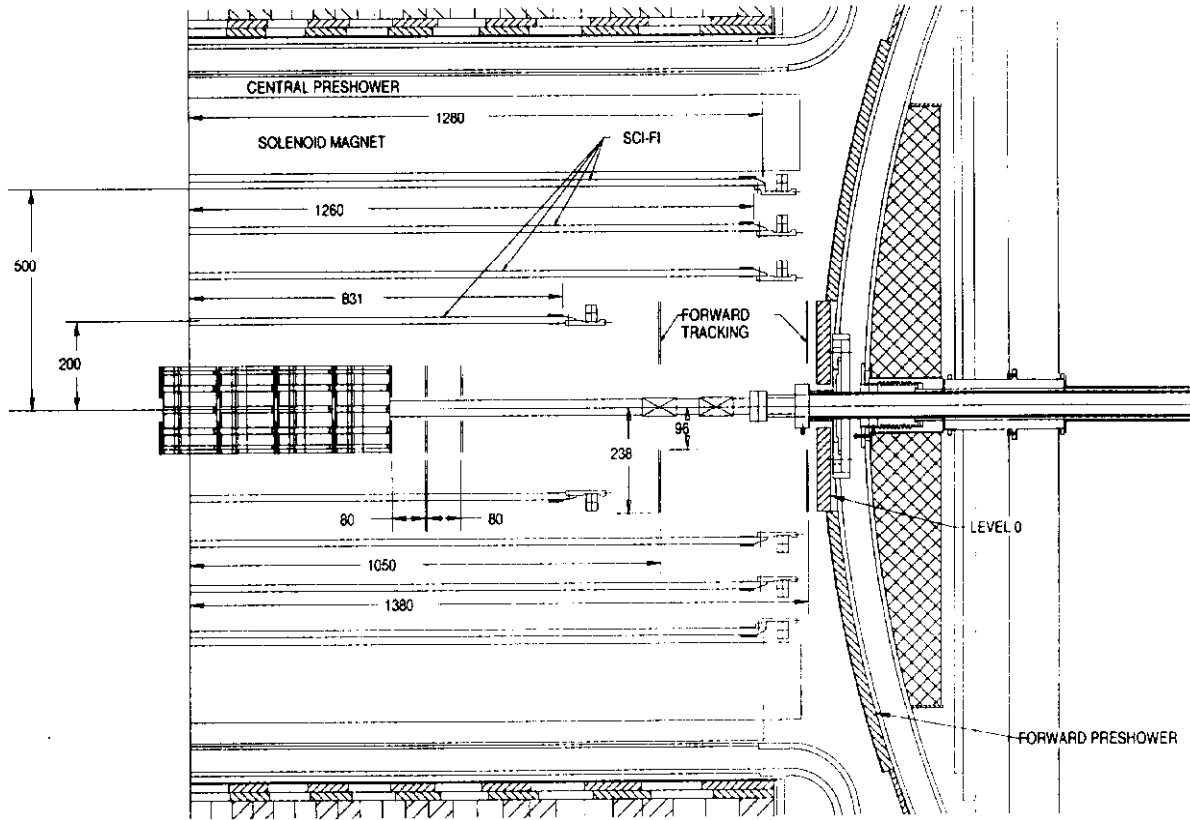


Figure 1. r-z view of DØ detector upgrade

detector upgrade.

2. Silicon Tracking

The silicon tracking system[4] is based on $50\ \mu\text{m}$ pitch silicon microstrip detectors providing a spatial resolution of approximately $10\ \mu\text{m}$ in $r\phi$. The high resolution is important to obtain good momentum measurement and vertex reconstruction. The detector consists of a system of barrels and interleaved disks designed to provide good coverage out to $\eta \approx 3$ for all tracks emerging from the interaction region, which is distributed along the beam direction with $\sigma_z \approx 25\ \text{cm}$.

The barrel has 7 sections, each 12 cm long and containing 4 layers. The first and third layers are made of single-sided detectors with axial strips and the second and fourth layers are made from double-sided detectors with axial and 2° stereo strips. The small angle stereo design provides good pattern recognition with a resolution in $r-z$ at the vertex of 0.5–1.0 mm, allowing separation of primary vertices from multiple interactions.

The detectors are ac-coupled – each strip has an integrated coupling capacitor and polysilicon bias resistor. This technology has been shown to be sufficiently radiation hard[6]. The front end read-

out chip (SVX II) has been prototyped in CMOS technology. It contains 128 channels, each channel comprising a double-correlated sampling amplifier, a 32-cell analog pipeline, and an analog-to-digital converter. The chip also contains sparse readout circuitry to limit the total readout time. The SVX II chips are mounted on a kapton high density circuit that is glued to the surface of the silicon detector. The detectors are mounted on beryllium bulkheads that serve as a support and provide cooling via water flow through beryllium tubes integrated into the bulkheads. The silicon tracker has a total of 837,000 channels.

3. Scintillating Fiber Tracker

The outer tracking is based on scintillating fiber technology readout by visible light photon counters (VLPCs) [3]. This decision was driven by this system's many performance strengths: excellent resolution and two track separation; superb tracking efficiency; and very fast time response providing information for level one trigger information. The tracker will consist of approximately 80,000 fibers configured into four superlayers placed at radii of 20, 30, 40, and 50 cm. Each superlayer contains four doublets that will

be arranged in an axial, +stereo, -stereo, axial configuration with the stereo angle set for each super layer to yield constant pitch ($\theta = 1.3$ to 3.3 degree). Each doublet consists of two layers of 830 μm multicladd scintillating fiber set at a fiber to fiber pitch of 870 μm . The two layers within the doublet are offset by one-half fiber spacing relative to each other. The doublets will be mounted on a carbon fiber/hexcell support cylinder with one axial layer mounted on the inner surface. This will provide a 1.5 cm separation between the axial doublets. Full GEANT Monte Carlo studies have shown that this geometry will provide 100% tracking efficiency in complex events, if the number of detected photons per mip is greater than 5 per doublet layer. They have also indicated that the tracking resolution should be approximately 120 μm .

The scintillation light from the fibers will be piped via 8m long clear fibers of 965 μm diameter to the VLPCs that will be located outside the tracking volume. We chose the VLPCs for the photodetector because of their good quantum efficiency ($\geq 60\%$), high gain (20,000+), and very fast response, $\tau_r \leq 100$ ps. The VLPCs are processed into arrays of eight 1 mm round pixels on a pitch of 1.05 mm. Figure 2 shows a typical multi-photoelectron pulse height distribution from a VLPC.

In order to fully test the basic concepts of this design, we have set up a cosmic-ray test consisting of a scintillating fiber tracker with approximately 3000 channels arranged in 3 full superlayers. [5] Data recorded over the past six months yield preliminary results that give a doublet photo-yield of approximately 19 (approximately four times what is required for full tracking efficiency) and a spatial resolution of approximately 140 μm . Figure 3 gives data for the doublet yield and Figure 4 presents the doublet and singlet efficiencies, including the effect from known dead channels.

4. Preshower

The preshower detector will be located in a 55 mm gap between the solenoid coil and the central calorimeter and will cover a region of pseudorapidity of $-1.3 \leq \eta \leq 1.3$. A tapered lead

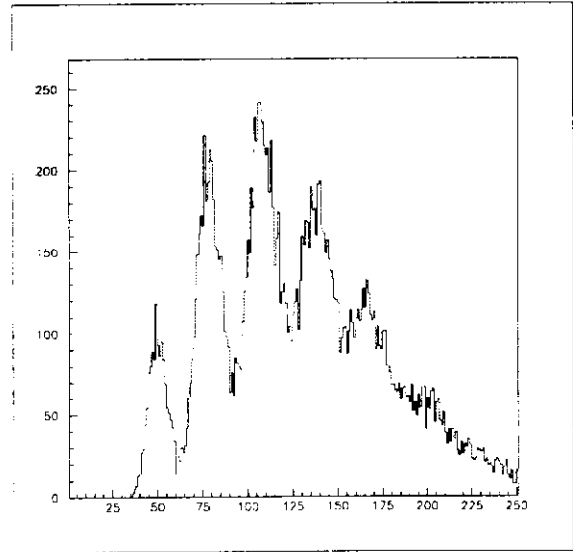


Figure 2. Typical multi-photoelectron spectrum from a VLPC

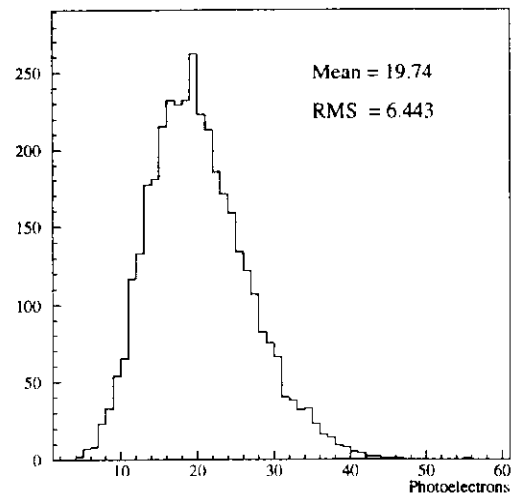


Figure 3. Doublet photoelectron yield

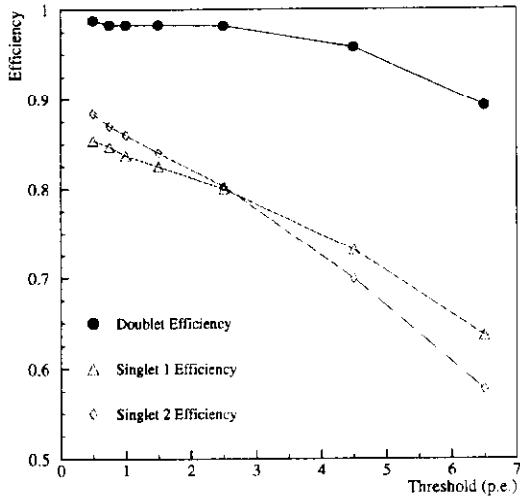


Figure 4. Singlet and doublet layer tracking efficiencies

absorber will be placed directly on the coil, such that the thickness of the lead plus coil will be approximately two radiation lengths for all particle trajectories within the above η range. We chose a scintillator based technology for the preshower detector and will utilize the VLPC readout system of the fiber tracker. Six layers of scintillator segmented into 5 mm cells and readout with wavelength shifting (WLS) fiber will be employed. The total number of channels in this system is approximately 7700. The scintillator layers are organized in $z-z$, $u-u$, and $v-v$ layers with the uv layers using a stereo angle of ± 20 degrees. The two layers in each doublet are offset by one-half cell spacing, as is done in the fiber tracker. We are investigating two implementations of the scintillator cell design: machined scintillator plate to form so-called “mega-tiles”; and individual cells of extruded scintillator with a hole down the center of the extrusion for the WLS fiber, see Fig. 5. As in the case of the fiber tracker, the optical signal from the WLS fibers will be piped to the VLPCs via 8m long clear fiber waveguides. We have per-

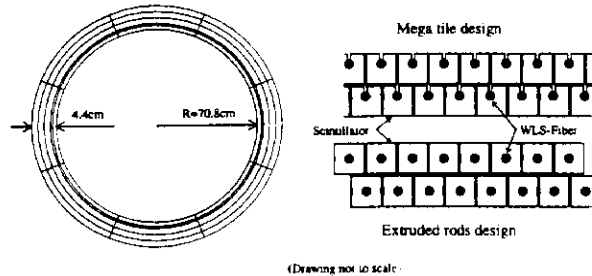


Figure 5. Cell geometry designs for the central preshower, mega-tile and extruded scintillator rod

formed extensive Monte Carlo studies with this detector, and they indicate a $\sigma_{R-\phi}$ spatial resolution of 1.0 mm and σ_{R-z} of 2.0 mm for 50 GeV/c electrons at $\eta = 1.0$. Test beam data from a prototype of this detector that used multianode phototube readout yielded, at 10 GeV/c, a pion rejection of 88% for an electron tagging efficiency of 85% and, at 50 GeV/c, yielded a 96% pion rejection for an electron tagging efficiency of 98%. The preshower detector along with E/p matching will enhance the $D\phi$ detector’s electron ID capabilities, even with the loss of the TRD.

5. Electronics and tracking trigger

The electronics system for the $D\phi$ upgrade will have a design similar to the current VME based system. We will use the SVX II as the front end device for the silicon and fiber trackers and the preshower detector. A precursor chip, amplifier/shaper/discriminator (ASD), will be used for the trigger channels (axial layers) of the fiber tracker and preshower detectors. It will receive analog signals from the VLPCs and provide a discriminator output for fast trigger pickoff and, in parallel, will provide an analog signal for the SVX

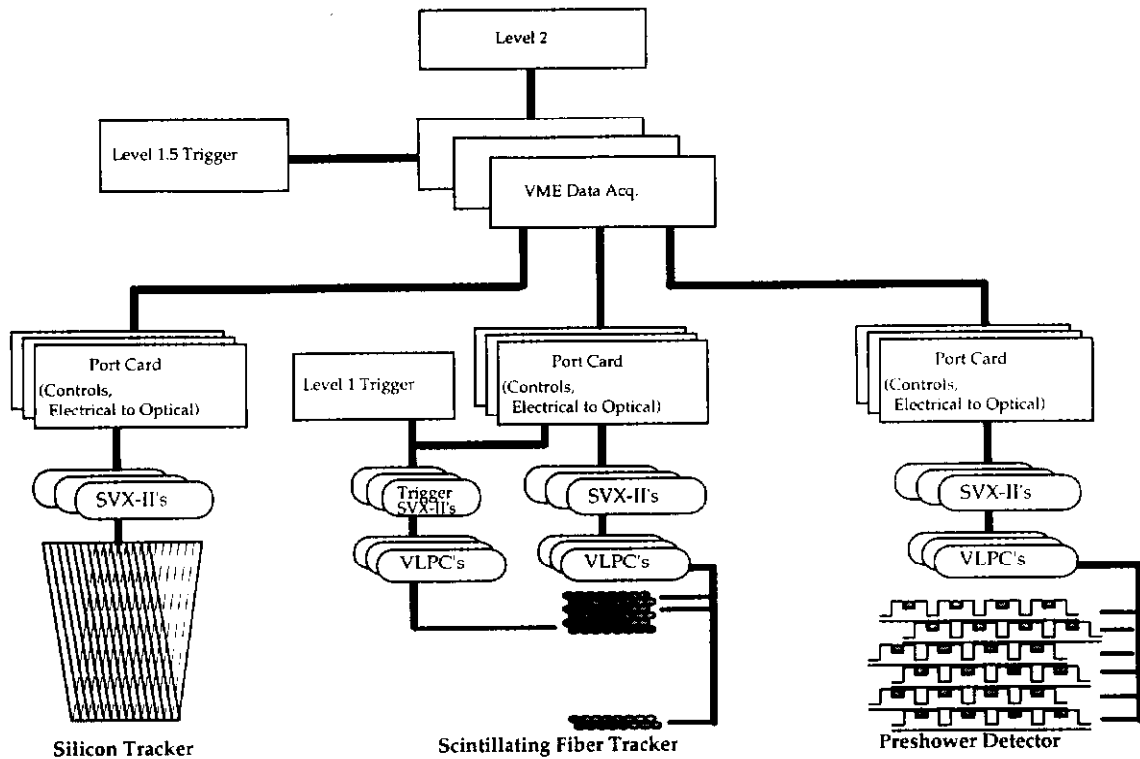


Figure 6. DØ upgrade electronics schematic

II. One Gb/sec fiber links will transmit data from the front end systems to the VME electronics. A schematic of the electronics system is given in Fig. 6. The axial layers of the fiber tracker will provide a level one tracking trigger. Hit information from individual fibers (from the precursor chip discriminator output) will be ganged in groups of 2,4,8, and 8 fibers for superlayers one through four, respectively. Vector centroids will be formed from hits in the two axial layers of each superlayer. Road finding logic (implemented in field programmable gate arrays, FPGAs) will then use this centroid information to find tracks. Figure 7 gives a schematic representation of this algorithm. In addition, the level one track trigger will incorporate information from the axial layers of the preshower detector (acting as "5th" layer) in order to tag tracks as electrons. A multi-level discriminator will be employed for the preshower detector so that we can tune the cut on the number of mips for an electron tag.

6. Detector Performance

The addition of the central solenoidal field provides important enhancements to DØ's physics capabilities: E/p matching for electron ID; charge sign determination; improved muon mo-

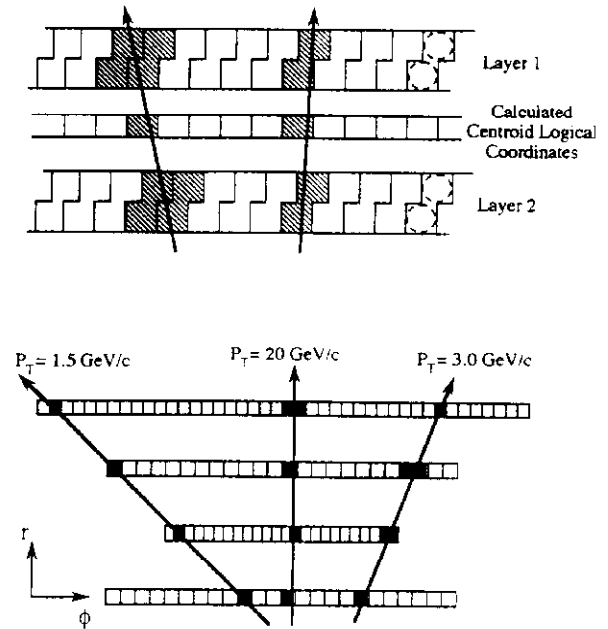


Figure 7. Ganging and track finding logic for level one track trigger

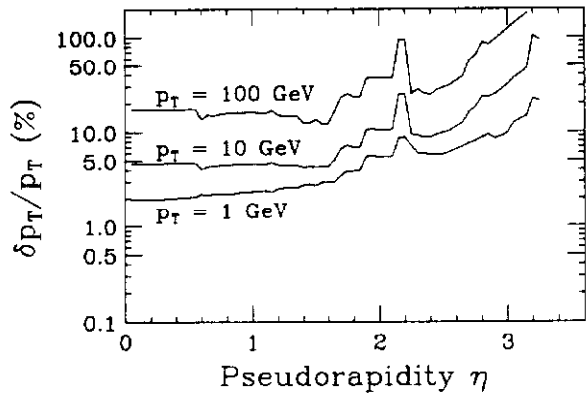


Figure 8. Transverse momentum resolution vs. pseudorapidity

momentum resolution; and in-situ calibration of the calorimeters. We have run full GEANT simulations of the upgrade detector's performance on representative events from $t\bar{t}$, electroweak, QCD, and b -quark physics channels. Figure 8 shows the momentum resolution for the proposed upgrade tracker using a realistic (non-ideal) field map. For 50 GeV/c, $\delta p_T/p_T$ varies between 8 and 40% for η between 0 and 3. The capability for charge sign determination represents a major enhancement to the DØ detector and will have a large impact on a number of physics studies. Figure 9 shows the two and three sigma level of sign determination in $Z \rightarrow \mu^- \mu^+$ events. From $J/\Psi \rightarrow \mu\mu$ Monte Carlo events, we have determined that the magnetic tracker yields a J/Ψ mass resolution of approximately 41 MeV/c². The silicon system in the upgrade tracker will provide the DØ detector with the capability to tag displaced vertices in $t\bar{t}$ and b -quark events. Simulations have shown that the proposed silicon system will give excellent impact parameter resolution over a large η range. The impact resolution is typically better than 20 μm for $\eta \leq 2$ and $p_T \geq 1$ GeV/c; see Fig. 10. Secondary vertex tagging will be a powerful tool for selecting top quark candidates via $t \rightarrow Wb$.

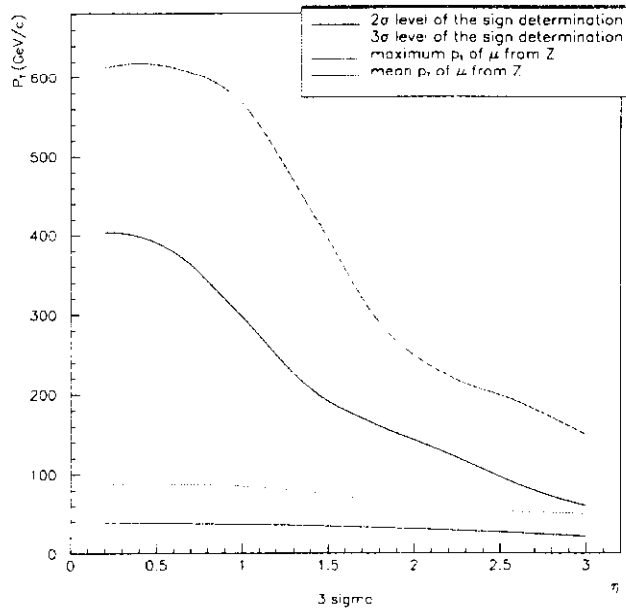


Figure 9. Charge sign determination in $Z \rightarrow \mu^- \mu^+$ events.

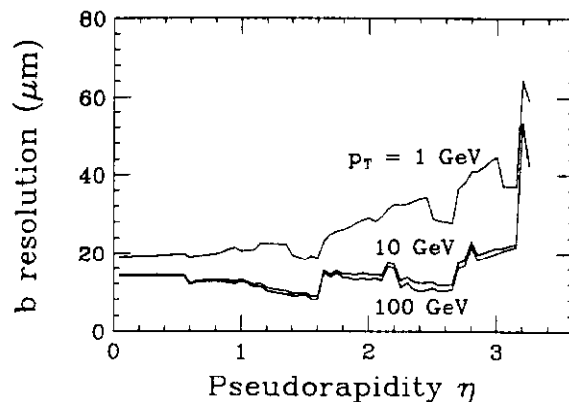


Figure 10. Two-dimensional impact parameter resolution vs. pseudorapidity.

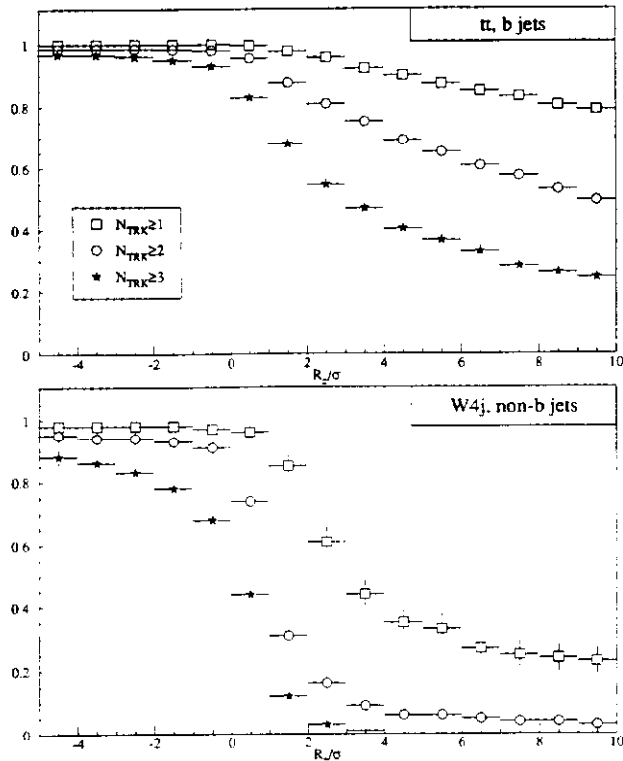


Figure 11. Fraction of events passing R_{\pm}/σ cut for $t\bar{t}$ events and $W + 4$ jet events.

We have performed a detailed GEANT study on a sample of $t\bar{t}$ and $W + 4$ jet events. We calculated a signed impact parameter, R_{\pm} , for tracks within jets and used it to define a significance cut: R_{\pm} divided by the impact parameter resolution σ for that event. For jets with ≥ 3 tracks, a significance cut of 3 yields a top quark tagging efficiency of approximately 50% with a background from $W + 4$ jet events of approximately 1%; see Fig. 11.

7. Physics opportunities

With upwards of one fb^{-1} of data available after the first run with the upgraded detector, precision measurements of the W boson and top quark mass will become important goals for the $D\phi$ experiment. With a sample size this large and with the capacity to perform in-situ energy calibration of the calorimeter, we expect that the upgraded detector can be used to measure the W mass to a precision of approximately $50 \text{ MeV}/c^2$. Measurement of the top quark mass will be one of the

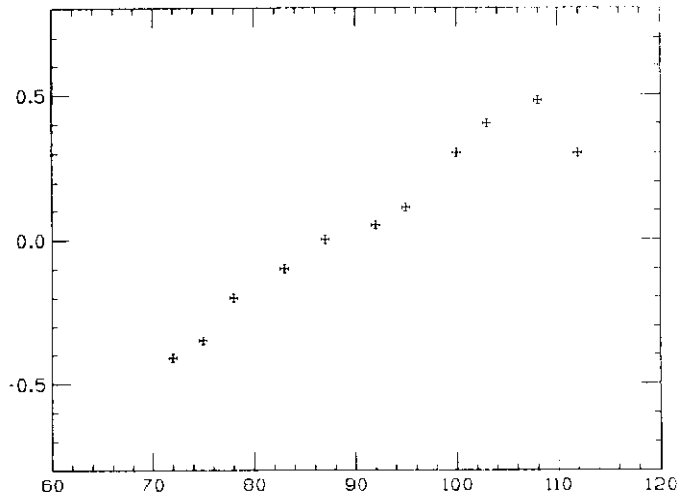


Figure 12. Variation of A_{FB} as a function of $m_{e^+e^-}$.

highest priorities for the upgraded detector. The silicon tracker will permit “tagging” of top quark candidates via the measurement of displaced secondary vertices from bottom quark decays, as shown above, and will result in a relatively clean sample of top quark candidates. With the expected integrated luminosity, we estimate that we will be able to measure the top quark mass to a precision of approximately 3 to 5 GeV/c^2 , using events in the lepton + jets channels.

In the electroweak physics sector, the upgraded $D\phi$ detector will have an excellent opportunity to measure the forward-backward asymmetry (A_{FB}) in Z boson decays to two leptons and will be able to determine $\sin^2\theta_W$ to a precision of ≤ 0.001 . In the $Z \rightarrow e^+e^-$ channel, the variation of A_{FB} due to $\gamma - Z$ interference can be measured as a function of the invariant mass, $m_{e^+e^-}$; see Fig. 12. These data should yield a measurement of $\sin^2\theta_W$ to a precision that will be competitive with LEP measurements.

Precise measurement of the parameters m_t , m_W , and A_{FB} will allow $D\phi$ to make detailed tests of the Standard Model and to search for possible new physics. The relationship among these parameters sets constraints on the Standard

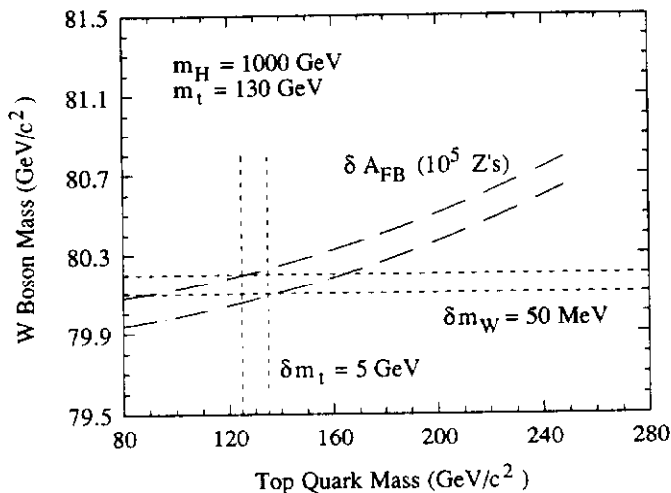


Figure 13. Plot of m_t vs m_W showing the expected precision on these mass measurements and the constraint from the measurement of A_{FB} .

Model, as is shown in Fig. 13, where we have assumed a top quark mass of $130 \text{ GeV}/c^2$ and a Higgs mass of $1000 \text{ GeV}/c^2$.

There are, of course, many other physics topics that are accessible with the upgraded detector and 1 fb^{-1} of integrated luminosity. The high p_T physics menu includes searches for supersymmetric particles; a search for a light charged Higgs via $t \rightarrow H^+ b$; a search for a neutral light Higgs via $H^0 \rightarrow b\bar{b}$; and the study of di-boson pair production. The copious production of b-quarks will allow for the study of a number of physics topics, including B spectroscopy and rare decays, B, mixing, and CP violation in the $B\bar{B}^0$ system.

8. Conclusions

The DØ detector upgrade program will be able to take full advantage of the physics opportunities afforded by the Tevatron upgrade. The detector designs for all major systems are at an advanced stage and simulation studies indicate that the detector will perform exceptionally well at peak luminosities as high as $1 - 2 \times 10^{32} \text{ cm}^{-2}\text{s}^{-1}$. A large scale prototype test for the scintillating fiber

tracker has given very encouraging results and shows the power of this emerging new technology. The upgraded DØ detector will be able to perform detailed studies of the Standard Model and will be in an ideal position to search for new physics.

I wish to thank my colleagues on the DØ upgrade project for many helpful discussions. In particular, I would like to thank J. Warchol, J. Ellison, R. Lipton, R. Ruchti, M. Johnson, and S. Glenn.

REFERENCES

1. DØ Collaboration, S. Abachi *et al.*, Nucl. Instrum. Methods **A338**, 185 (1994).
2. DØ Collaboration, "The DØ Upgrade", 18 October 1990; DØ Collaboration, "E823 (DØ Upgrade) - Step I and Beyond", DØ Note 1421, May 1992; DØ Collaboration, "E823 (DØ Upgrade) - $D\theta_\beta$ ", DØ Note 1733, May, 1993; DØ Collaboration, "E823 (DØ Upgrade) - "B Tagging and Electron Identification," DØ Note 2054, February, 1994.
3. M.D. Petroff *et al.*, Appl. Phys. Lett. **51**, (1987) 406.; M.D. Petroff and M. Atac, IEEE Trans. Nucl. Sci., **36**, No. 1 (1989) 158.
4. DØ Collaboration, "DØ Silicon Tracker Technical Design Report", DØ Note 2169, July 1994.
5. See D. Adams *et al.*, Cosmic ray test results of the DØ prototype scintillating fiber tracker; and D. Adams *et al.*, First large sample study of visible light photon counters (VLPCs), these proceedings.
6. D. Pitzl *et al.*, Nucl. Phys. B (Proc. Suppl.) **23A**, 340 (1991); H.J. Ziocck *et al.*, IEEE Trans. Nucl. Sci. **NS-38**, 269 (1991).